



**HAL**  
open science

# Litharge from El Centenillo and Fuente Espi: A Geochemical and Mineralogical Investigation of Spanish Silver Processing in the Sierra Morena

P. Krause, S. Klein, C. Domergue, Chr. Berthold, N. Jöns

► **To cite this version:**

P. Krause, S. Klein, C. Domergue, Chr. Berthold, N. Jöns. Litharge from El Centenillo and Fuente Espi: A Geochemical and Mineralogical Investigation of Spanish Silver Processing in the Sierra Morena. *Metallography, Microstructure, and Analysis*, 2023, 12 (2), pp.262-275. 10.1007/s13632-023-00940-8. hal-04257145

**HAL Id: hal-04257145**

**<https://univ-tlse2.hal.science/hal-04257145v1>**

Submitted on 22 Feb 2024

**HAL** is a multi-disciplinary open access archive for the deposit and dissemination of scientific research documents, whether they are published or not. The documents may come from teaching and research institutions in France or abroad, or from public or private research centers.

L'archive ouverte pluridisciplinaire **HAL**, est destinée au dépôt et à la diffusion de documents scientifiques de niveau recherche, publiés ou non, émanant des établissements d'enseignement et de recherche français ou étrangers, des laboratoires publics ou privés.



Distributed under a Creative Commons Attribution - NonCommercial 4.0 International License



# Litharge from El Centenillo and Fuente Espi: A Geochemical and Mineralogical Investigation of Spanish Silver Processing in the Sierra Morena

P. Krause<sup>1,2</sup> · S. Klein<sup>2,3</sup> · C. Domergue<sup>4</sup> · Chr. Berthold<sup>5</sup> · N. Jöns<sup>1</sup>

Received: 1 October 2022 / Revised: 23 December 2022 / Accepted: 3 February 2023 / Published online: 28 April 2023  
© The Author(s) 2023

## Abstract

Galena is treated as the most important silver ore in antiquity and especially in Roman mining history, but many other silver mineralisation and phases occur in the Earth's crust that also contain valuable amounts of silver for exploitation. This study addresses the silver-containing sulfosalts and how to decide between the alternative ores when only metallurgical remains are preserved and the mining context is not evident. Numerous samples of ore minerals, slags, lead metal and stones were collected by one of us (C. Domergue) over several years in the Spanish Sierra Morena, including two Roman foundry sites: Cerro del Plomo and Fuente Espi, both in the mining district of Linares-La Carolina. Cerro del Plomo is closely associated with lead-bearing ore veins near the foundry, while the mines that supplied Fuente Espi with lead ore have not yet been archaeologically explored. The metallurgical remains from the two foundries were analysed for their microstructure, mineralogy and phase composition using microscopy, electron microprobe analysis and X-ray diffraction. It was hoped that the litharge in particular would provide information about the ores used. Metal inclusions of copper and lead were identified, both still containing some silver. The cooling history and stratigraphy of the litharge cakes were developed and parallels drawn with earlier cupellation models. The litharge cakes from Cerro del Plomo and Fuente Espi are comparable in terms of microstructure and phase composition. Chemical and isotope analysis will follow and be the subject of a separate publication.

**Keywords** Archaeometallurgy · Lead ore · Galena · Foundry · Litharge · El Centenillo · Cerro del Plomo · Fuente Espi · La Carolina · Sierra Morena · Spain · Roman

---

This invited article is part of a special topical issue of the journal *Metallography, Microstructure, and Analysis* on Archaeometallurgy. The issue was organized by Dr. Patricia Carrizo, National Technological University – Mendoza Regional, and Dr. Omid Oudbashi, Art University of Isfahan and The Metropolitan Museum of Art, on behalf of the ASM International Archaeometallurgy Committee.

---

✉ P. Krause  
Paul.Krause@ruhr-uni-bochum.de

<sup>1</sup> Institut für Geologie, Mineralogie und Geophysik, Ruhr-Universität Bochum, Universitätsstrasse 150, 44801 Bochum, Germany

<sup>2</sup> Forschungsbereich Archäometallurgie, Deutsches Bergbau-Museum Bochum, Am Bergbaumuseum 31, 44791 Bochum, Germany

## Introduction

From archaeological point of view, the silver-rich lead ore, galena, is of outstanding importance as the natural geo-resource for silver. This is almost independent of the archaeological period or the region that is the focus of each study. However, this view on silver is very one-dimensional from a mineralogical point of view, since very large variation of silver ore exists in different geological formations [1]. Paragenesis is known with several elements (Te, Sb, Au,

<sup>3</sup> Institut für Archäologische Wissenschaften, Ruhr-Universität Bochum, Am Bergbaumuseum 31, 44791 Bochum, Germany

<sup>4</sup> Laboratoire TRACES (UMR 5608 CNRS), Université Toulouse-Jean Jaurès, 5 Allées Antonio Machado, 31058 Toulouse Cédex 9, France

<sup>5</sup> Competence Center Archaeometry – Baden-Wuerttemberg (CCA-BW), Eberhard Karls-Universität Tübingen, Wilhelmstraße 56, 72074 Tübingen, Germany

Cu, As, Hg, S, Cl) and minerals, especially the co-existence with sphalerite (Zn), galena (Pb), lead sulfosalts, and silver minerals. Primary silver mineralisation occurs worldwide in complex hydrothermal veins as sulphide minerals, sulphosalts or Bi–Co–Ni–Ag (Schneeberg–Kongsberg type) or Ag–Co–Ni–Bi–As(-U) (“five-element”) associations, as galena-hosted Pb from massive sulphide deposits and sub-volcanic settings (Au–Ag) [2]. Secondary silver mineralisation forms in oxidation zones, e.g. as jarosite, a group of hydroxy-sulphate multi-element sandy soils [3].

It is therefore overdue to study the metallurgical remains of lead silver smelting in more detail archaeometrically, especially if the remains are decoupled from the supplying mine, further to find clues as to whether galena or other silver minerals were used to produce silver metal. The bouquet of silver minerals and parageneses may also have resulted in different smelting techniques. Even co-smelting of mixtures of sulphide and oxide silver minerals may have been practiced [4], as the mineralogy of silver shows high potential for this process. Co-smelting is much easier to perform than the laborious roasting and sulphide smelting steps [4], and it does not require pre-roasting of sulphide ore and is a self-operating process depending on the thermodynamic conditions (e.g. the free energy of the reaction at certain temperature). Litharge cakes are hence the most promising material for this objective, as several oxides (e.g. Cu, Zn, Fe, Mn, Sn, Sb, As, also Ca, Ba, Mg) are absorbed together with lead oxide by the collecting clay, which can then better reflect the mineralogy of the ore than other metallurgical by-products.

The term “litharge” is originally derived from the Greek words *lithos* (stone) and *argyros* (silver). In the first century AD, the term was used by Pedanios Dioskourides in his *De Materia Medica* and by Pliny the Elder in his *Naturalis Historia* [5]. Several German names are (were) used; presumably, the most common one is “Bleiglätte” [6]. Others were more specifically in context to pigments and paintings (“Königsgelb”, “Bleigelb”, or “Goldglätte”). Although they are now classified as toxic, the red and yellow pigments are still produced as pigments today [7]. Litharge was also used during Medieval times in medicine [5]. Mineralogically, litharge is a modification of divalent lead monoxide Pb(II)O. Lithargite or litharge,  $\alpha$ -Pb(II)O, is intense red as a powder, tetragonal and stable at room temperature. Massicotite or massicot, the orthorhombic  $\beta$ -Pb(II)O, is almost luminescent sulphur- to orpiment-yellow as a powder and forms from  $\alpha$ -Pb(II)O as a metastable phase at transition temperature of 488 °C [8]. The process of transformation from the high- to low-temperature modification of Pb(II)O is reversible, but the transformation takes place fairly during cooling. Rapid cooling therefore preserves the high-temperature phase, whereas slowly cooling causes the two modifications to co-exist. In nature, litharge occurs as massive to

earthy oxidation product of lead sulphide minerals (galena) in gossans or mine dumps, which consist mainly of litharge and only to a small extent of massicot [9]. Metallurgically, litharge forms as a waste product during the cupellation of silver as solid lumps or brick-like [5], or accidentally in metallurgical setting [10, 11]. It was also described more generally as a product of galena roasting [12]. In fact, litharge cakes are produced in the cupellation process by overflowing of the liquid litharge, which is then collected in a crucible or collecting pit [5, 13, 14]. To make the process work, a porous, calcium-rich clay is needed, which is mixed with plant ash, bone ash or a mixture of both to absorb the litharge and impurities in the process [10]. It hence comprises a heterogeneous mixture of clay components with lead oxide [15]–[20]. On top of the lead oxide-clay mass, “bubbles of carbonic acids” develop [19]. This way, separation and purification of silver can be reached in a single step. Synthetically, massicot can be produced by heating a precursor, e.g. cerussite, which decomposes between 130 and 470 °C [22]. Parallel to nature and metallurgy, mixtures of  $\alpha$ - and  $\beta$ -Pb(II)O can be reproduced experimentally [23, 24]. Great care must be laid on the procedures in the laboratory, because massicot was reported to convert back to litharge by grinding the litharge cake [23]. Questions arise, (1) how the PbO modifications interact with clay component, (2) in which of the components of the litharge cakes lost silver is trapped, and (3) whether the elemental composition of the silver can be used as a fingerprint for the ore smelted.

## Archaeological and Geographical Setting

The samples presented in this paper are from two sites in the eastern Sierra Morena, in the province of Jaén (Spain). These are two lead foundries from the Roman period, both located in the vicinity of silver galena mines in the district of Linares-La Carolina. The first one, Cerro del Plomo, is located 20 km north of the town of La Carolina, in the middle of the mountains, on the territory of the El Centenillo mine, below the mining settlement of the contemporary period (nineteenth and twentieth centuries). It covered the top of a hill. In 1968 and 1969, one of us (C. Domergue) carried out archaeological excavations there, which revealed that this foundry had experienced two distinct periods of activity, first in the second and first centuries BCE and then, in the first and second centuries CE [25, 26]. Lead ores (galena) were processed here, from which silver-rich lead was extracted. This lead was subjected to cupellation, which allowed the silver to be extracted. During this process, the lead was transformed into oxide (litharge), which could be melted down again to obtain de-silvered lead (or soft lead), which was commonly used in Roman times, primarily for making pipes for water distribution in cities. The location

of the Cerro del Plomo foundry, opposite the entrance to a mining gallery (Socavón Don Francisco) of a rich vein in El Centenillo, the Mirador vein, leads us to believe that this metallurgical factory may have given priority to processing the galena from this vein. However, as other finds on the same site suggest, ore from other mines must also have been processed here. During the excavations, numerous samples of galena, lead and litharge were collected, sometimes from well-dated occupation levels. Many of these samples were put to immediate use and were the subject of quantitative and semi-quantitative elemental analyses [25]. Those that remained constitute the material studied in this article.

At about the same time that the archaeological excavations of Cerro del Plomo were taking place, in the vicinity of La Carolina, between the cemetery and the entrance to the town, at the place called Fuente Espi, important earthworks were being carried out in view of the construction of a showroom for the Santana car company. This work uncovered the remains of an important lead foundry from the Roman period, which was active in the first century CE [26]. Nothing was preserved, and no archaeological excavations could be carried out, but samples of galena, lead, litharge, and slag were collected. These are among those presented below. Unlike Cerro del Plomo, which was obviously linked to the El Centenillo mine, the Fuente Espi foundry was not located in the territory of a particular mine. Specifically, it was located in the heart of a mining district, not far from mines such as El Castillo, La Torrecilla, Los Guindos and had to process the lead ore from the latter.

Objects found in these two foundries attract attention. They are used as lead seals, which had been used to seal bundles carrying material considered valuable enough to justify such care [27]. They bear various inscriptions, in particular the abbreviation *S.C.*: it was thought to be developed into *Societas Castulonensis*, *Castulo* from the name of an important ancient city in the region, Castulo. As for the nature of the materials thus delivered to the foundries, it has been assumed, among other interpretations, that they could be ore concentrates, transported from other mines to be processed in one or other of these two foundries. If this is the case, the samples (galena, lead, litharge, slag) should indicate different origins.

## The Material

The samples originate from the private collection from long years of research of one of us (C. Domergue). They were handed over years ago to TRACES (CNRS laboratory at Toulouse University) and stored in a dedicated room belonging to the metal team (responsible Ch. Rico and S. Baron). The selection of samples has been made on site with special focus on litharge (Table 1 and Fig. 1) and ore from the Sierra Morena.

## Elemental and Phase Analytical Methods

From the Cerro del Plomo site, samples NA5, 5, and 53 (two thin sections: 53.1 and 53.2) were prepared as thin sections and were micro-analysed using reflected light microscopy. From Fuente Espi - La Carolina samples were equally prepared from litharge cakes numbers 63b, 64 and 67.

Reflected light microscopy was performed on the sections using a Zeiss Axiophot microscope with an AxiCam Camera. For electron probe microanalysis (EPMA), a Cameca SX Five FE electron microprobe at Ruhr-Universität Bochum was available. The following crystals were used: LTAP, for Na, Mg, Al, Si; LPET for K, P, S; LLIF for Ca, Ag, Pb, Mn, Ni, Zn; and LIF for Fe and Cu. Following standards were used as available in the microprobe laboratory: Jadeite, Diopside, Spessartine, Orthoclase, Fluorapatite, FeS<sub>2</sub>, Mn, Ni, Cu, ZnS, Ag<sub>2</sub>Te, PbS. Measuring conditions were 20 keV acceleration voltage and 40 nA probe current. To obtain high spatial resolution, a fully focused beam was used. X-ray diffraction (XRD) was used for phase differentiation between litharge and massicot in the sampled litharge cakes. Different zones of the cake were carefully separated with a chisel and ground to powder with an agate mortar. XRD phase analysis was performed for samples 53 and 63b at the CCA-BW, Tübingen using a Bruker D8 advance powder diffractometer equipped with a Cu-sealed tube (40 kV/20 mA), a Göbel mirror optics, a 0.2 mm divergence slit, a fixed knife edge to suppress air scatter and a VÅNTEC 1-detector in scanning mode [28]. Measurement

**Table 1** Inventory list of selected material from the Toulouse collection. [NA = information not available]

Region 1	Region 2	Site	Mine	Sample	Description 1	Description 2	Description 3	Dating
Sierra Morena	Jaen	Cerro de Plomo	El Centenillo	NA 5	Litharge	Sondage P1 layer II	NA	NA
Sierra Morena	Jaen	Cerro de Plomo	El Centenillo	5	Litharge	Fonderie site	NA	NA
Sierra Morena	Jaen	Cerro de Plomo	El Centenillo	53	Litharge	Fonderie site	NA	NA
Sierra Morena	Jaen	Fuente Espi	La Carolina	63	Litharge	NA	NA	1 ct. CE
Sierra Morena	Jaen	Fuente Espi	La Carolina	67	Litharge	NA	NA	1 ct. CE
Sierra Morena	Jaen	Fuente Espi	La Carolina	64	Litharge	NA	NA	1 ct. CE

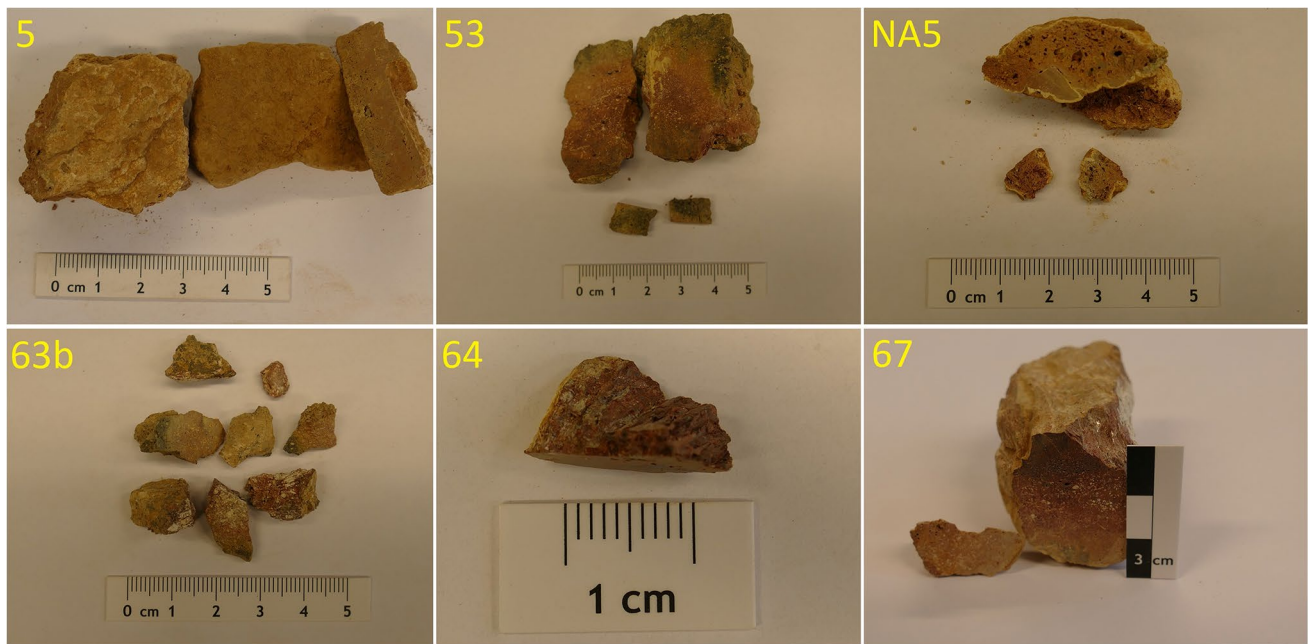


**Fig. 1** Litharge samples from Cerro del Plomo (NA 5, 5, 53) and Fuente Espi (63, 64, 67) as selected for analysis

range was  $2\text{--}70^\circ 2\theta$ , and step size was  $0.008^\circ$  and step time 405 s. For better crystallite statistics, the samples were rotated during the measurement. The PDF-2 database from ICDD (International Center of Diffraction Data) was used for phase identification.

## Results

### Microscopy of the Litharge Cake Samples

By cutting the litharge cakes from both sites in slabs, a gradual change in colour from red to yellow material can be observed. Under the stereomicroscope, several compositional zones can be further differentiated: A dark red (I) and a red zone (II), a reddish zone (III) in transition between red and yellow areas of the cross sections, and a yellow to brownish–black zone (IV) in the yellow area of the cross sections. The boundary between zone I and II is very sharp and distinct, whereas between II, III and IV the transitions are smooth. In Fig. 2, the different zones are indicated by yellow lines. All four zones were observed in samples 5 (Cerro del Plomo), 63b and 64 (Fuente Espi). In samples 53 (53.2; Cerro del Plomo) and 64 (Fuente Espi), the yellowish hue of the reddish zone III is evident. In NA5 (Cerro del Plomo), zone II could not be determined macroscopically, but was later microstructurally defined.

The main objective of the microscopy was a detailed mineralogical description of zones I to IV (Fig. 3). The

dark red zone I was observed in all samples except sample 53 (53.2; Cerro del Plomo). This zone is characterized by lath-like crystals up to  $> 1$  mm in length. The reflective colour is creamy white to light grey with strong red to orange internal reflections. They form a kind of crystallite framework, sometimes in preferred orientation. Especially in sample 64 (Fuente Espi), the lath-like crystals are overprinted by alteration. The interstices between the lath-like crystals are filled by a phase with grey reflection colour. High pore volume contributes to the structure. In samples 53 (53.1; Fuente Espi) and 67 (Cerro del Plomo), small metal inclusions of pink reflective colour with a size  $< 50 \mu\text{m}$  were identified. Based on their microscopic characteristics, they consist of metallic copper. The boundary between zones I and II is sharp and distinct. The phase composition of red zone II becomes generally more complex compared to zone I. Zone II is again porous and is characterized by a crystal framework, but here, the creamy white crystals with red to orange internal reflection tend to be smaller in size, acicular in shape and mostly occur weathered (Fig. 3d). They decrease in volume portion (observed in samples 5 (Cerro del Plomo), 53 (53.1 and 53.2, Cerro del Plomo) and 63b (Fuente Espi)) in favour to a grey matrix, in which individual phases are almost impossible to recognize. The transition between zones II and III is smooth. In Zone III, the proportion of the white acicular crystals decreases further in favour of the grey matrix. The transition from zone III to zone IV is again smooth. White acicular crystals are absent in zone IV, but the white phase appears as xenomorphs. Various phases with a grey reflection colour dominate zone IV. There is a



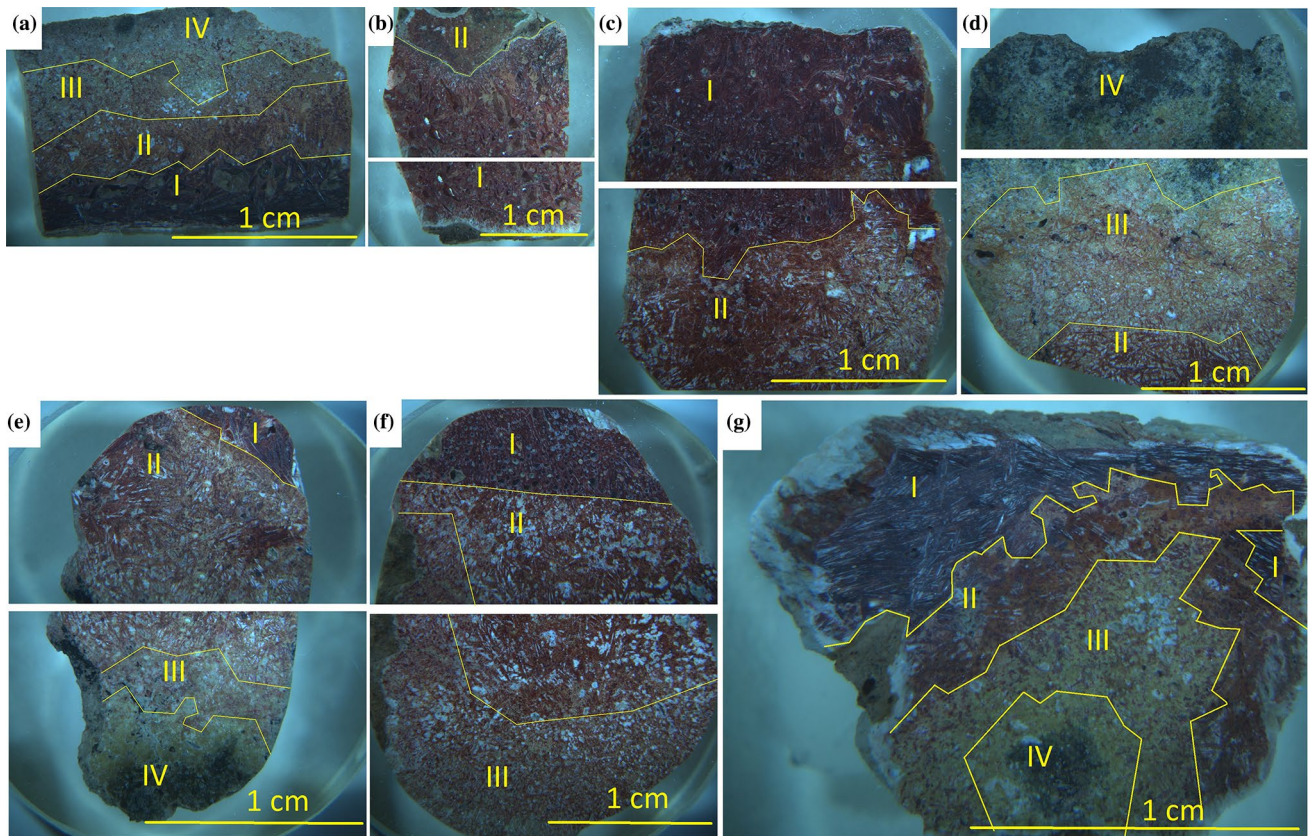


**Fig. 2** Litharge samples observed with the stereomicroscope. (a) Sample 5. (b) Sample NA5. (c) Sample 53.1. (d) Sample 53.2. (e) Sample 63b. (f) Sample 67. (g) Sample 64

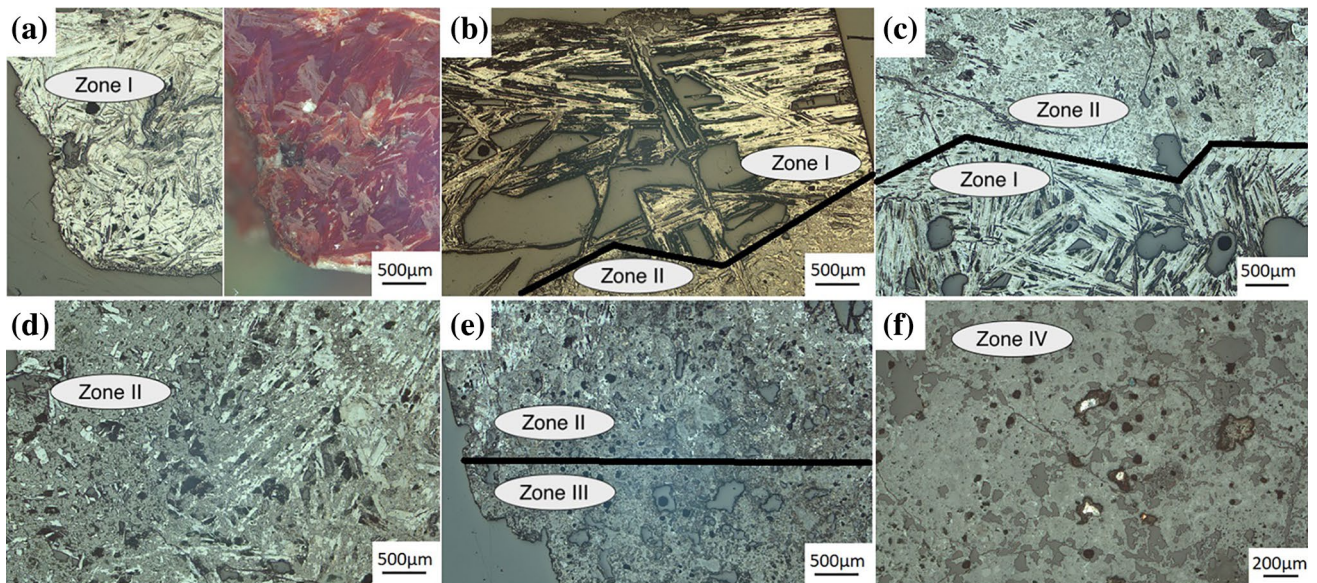


**Fig. 3** (a) Zone I with lath-like white crystals having red to orange internal reflections. (b) Zones I and II with sharp and distinct boundary (black line). (c) Visible change of microstructure between zones I and II in sample 53.1. (d) Zone II with white acicular crystals and

increasing grey phase. (e) Zones II and III with smooth transition. (f) Zone IV with metal inclusions in a matrix of grey phases (sample 53.2). Acicular crystals are absent

**Table 2** Comparison of PbO, Al<sub>2</sub>O<sub>3</sub>, SiO<sub>2</sub>, and FeO in phases A-C

	PbO			Al <sub>2</sub> O <sub>3</sub>	SiO <sub>2</sub>	Feo
	Phase A	Phase B	Phase C			
Minimum value	94.08	70.21	83.34	0.42	1.85	0.44
25%-Quantile	99.82	97.48	90.65	0.78	3.52	2.33
Median	99.90	99.06	91.15	1.02	3.95	3.21
Average	99.78	96.97	90.54	1.19	4.53	3.47
75%-Quantile	99.93	99.55	91.62	1.41	5.05	4.03
Maximum value	99.98	99.96	92.20	4.46	11.36	10.10

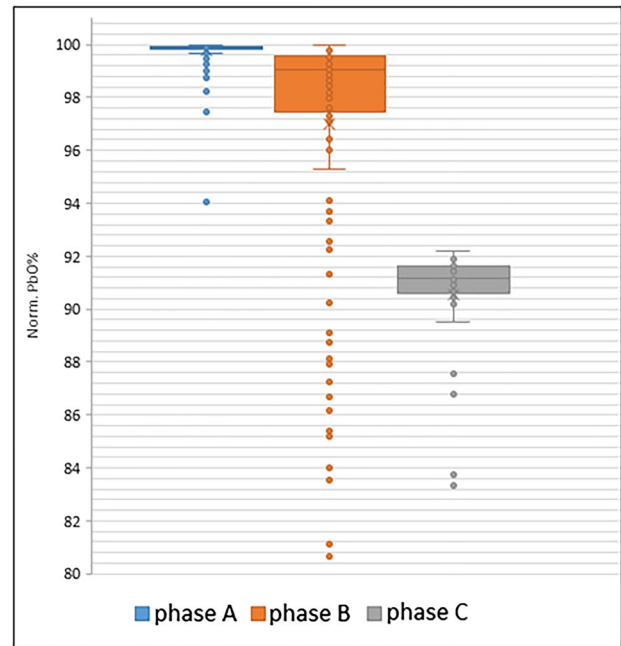


**Fig. 4** Box-whisker diagram showing the normalized PbO wt.% in phases A, B and C. The median Pbo content decreases from phase A to C

tendency for the proportion of the white phase to continuously decrease from zone I to zone IV.

Metal inclusions are observed in all samples. In samples 5, 53 (53.1 and 53.2; Cerro del Plomo), and 67 (Fuente Espi), angular inclusions < 50 μm in size and with a pink reflective colour can be identified. They occur preferable in zones II to IV. In samples NA5 (Cerro del Plomo), 53 (53.2) and 63b (Fuente Espi), metal inclusions with a striking white colour were also spotted (Fig. 3 f). These are surrounded by black to dark grey rims of a different phase.

Microscopically, no differentiation between the samples from the two foundries Cerro del Plomo and Fuente Espi can be made. Equal in Cerro del Plomo and Fuente Espi litharge cakes are the four different zones that vary from dark-red over red to reddish and finally, yellow-brownish black. The dark red zone comprises lath-like greyish-white crystals and another open-space-filling phase characterized by a medium to light grey reflection colour. From the dark red (I) to the red zone (II), a sharp boundary is observable. Visibly smaller, acicular white crystals in a greyish-white matrix characterize the red zone (II), and a gradually transition to the reddish zone (III) is characteristic. The reddish zone (III) consists of a grey matrix with metal inclusions (Cu, Pb). In the zones II and III, the needle-like crystals occur rarely and mostly, they are characterized by alteration (Fig. 3b). In zone IV, the needle-like phase is absent and the particles with a white reflection colour lost their



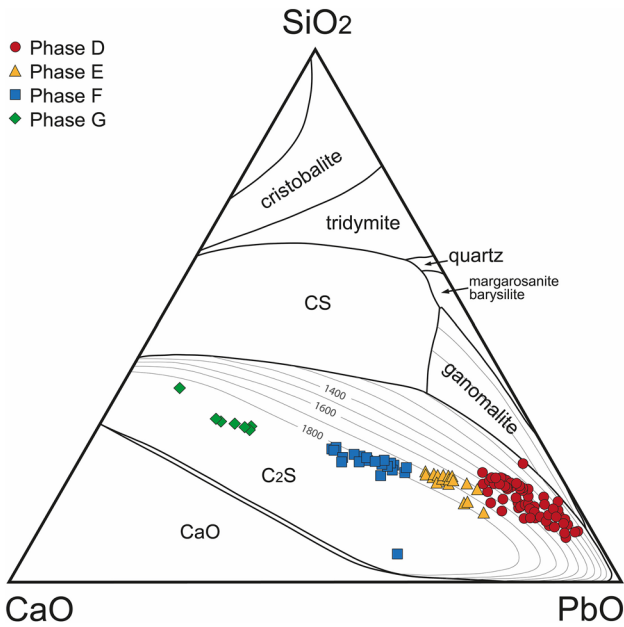


**Fig. 5** Phase diagram SiO<sub>2</sub>-CaO-PbO. The Ca–Si–Pb–O rich phases D to G plot in the C<sub>2</sub>S stability field and along temperature isochrones. Phase D matches the lowest temperature isochrone starting at 1100 °C and neighbouring the ganomalite field. Increasing theoretical temperatures result for phases E–G (according to liquidus projection of the “PbO”-CaO-SiO<sub>2</sub> system [24]; C<sub>2</sub>S = (Ca<sub>1-x</sub>Pb<sub>x</sub>)<sub>2</sub>SiO<sub>4</sub>), although this cannot meet the practical temperatures achieved in the furnace

recognizable idiomorphic form. Various phases with grey reflection colour predominate in zone IV.

**Electron Microscopy**

Phase identification with electron microprobe analysis focussed on the phase composition of the lath-like to acicular phase, the various grey phases and the metal inclusions.

**Lead-Rich Phases**

Three major compositions of PbO were identified (Table 2), in which the lead content decreases continuously (Fig. 4): Phase A is the purest PbO (99.90 wt.%). It represents the white lath-like to acicular phase in zones I-II. In zones II and III, phase A forms a complex BSE-white to grey matrix associated with additional phases. In samples NA5, 53 (53.2) from Cerro del Plomo and 63b from Fuente Espi, phase A also forms the rim around metallic inclusions. Phase B comprises of 99.06 wt.% PbO with contribution of CaO and SiO<sub>2</sub>. It fills the interstitial gaps between the laths in zone I as observed in samples 5 and 53 (53.1) from Cerro del Plomo, and 63b and 64 from Fuente Espi. Phase C has the lowest PbO content of the three (91.15 wt.%) with increased contents of Al<sub>2</sub>O<sub>3</sub> (1.40 wt.%), SiO<sub>2</sub> (3.95 wt.%) and FeO

**Table 3** Normalized standard oxides of phases D-G (the Ca–Si–Pb–O phases) and H-M (the Si–Pb–O phases with variable K, Al, Mg, Ca) within the 25%–75% quantile [in weight percentage; <0.xx = below detection limit; “Samples” = observed in]

	PbO	SiO <sub>2</sub>	Al <sub>2</sub> O <sub>3</sub>	CaO	MgO	K <sub>2</sub> O	Na <sub>2</sub> O	P <sub>2</sub> O <sub>5</sub>	CuO	FeO	Samples
	Norm. wt.% from 25%-quantile to 75%-quantile										
Phase D	70.80–78.50	12.67–18.12	0.11 – 0.65	6.89–10.02	0.04 – 0.30	< 0,02	< 0,04–0,05	< 0,03–0,30	< 0,09–0,13	< 0,07–1,81	All samples
Phase E	59.91–62.28	18.41–19.00	0.04–0,06	18.64–20.13	0.02–0,04	0,04–0,27	< 0,04–0,04	0,03–0,53	< 0,09	< 0,07	NA5, 53, 63b, 64, 67
Phase F	40.39–47.24	21.36–22.77	0,04–0,1	27.02–32.20	0,03–0,06	0,09–0,24	0,04–0,10	0,10–0,23	< 0,09	< 0,07	63b, 64, 67
Phase G	18.95–24.21	28.50–29.75	0,02–0,03	46.13–48.88	0,03–0,04	0,12–0,31	0,13–0,18	0,51–0,85	< 0,09	< 0,07	67
Phase H	64.31–68.27	9.55–11.18	12.55–15.71	6.08–7.18	0,35–0,70	0,07–1,07	0,13–0,28	< 0,03–0,06	< 0,09	0,09–0,18	53.2, 63b, 67
Phase J	82.31–83.90	10.41–13.44	2.31–5.08	0.11–1.04	< 0,02–0,24	< 0,02–0,06	< 0,04–0,06	< 0,03–0,06	< 0,09–0,19	< 0,07–0,66	5, 53.2, 63b, 64
Phase K	24.49–35.32	19.15–23.94	13.17–17.51	23.115–28.51	3.09–5.13	0,02–0,13	0,19–0,36	< 0,03–0,03	< 0,09–1,35	0,87–2,44	63b, 64
Phase L	48.55–55.91	19.73–21.52	0.16–0,45	11.77–17.22	11.02–11.33	< 0,02	< 0,04–0,07	0,31–0,37	0,09–0,19	0,08–0,34	63b, 67
Phase M	7.44–21.80	31.28–36.97	24.55–30.48	< 0,02–0,55	0.08–0,22	18.66–23.83	0.66–0,75	< 0,03–0,03	< 0,09	0.15–0,58	53.2, 63b



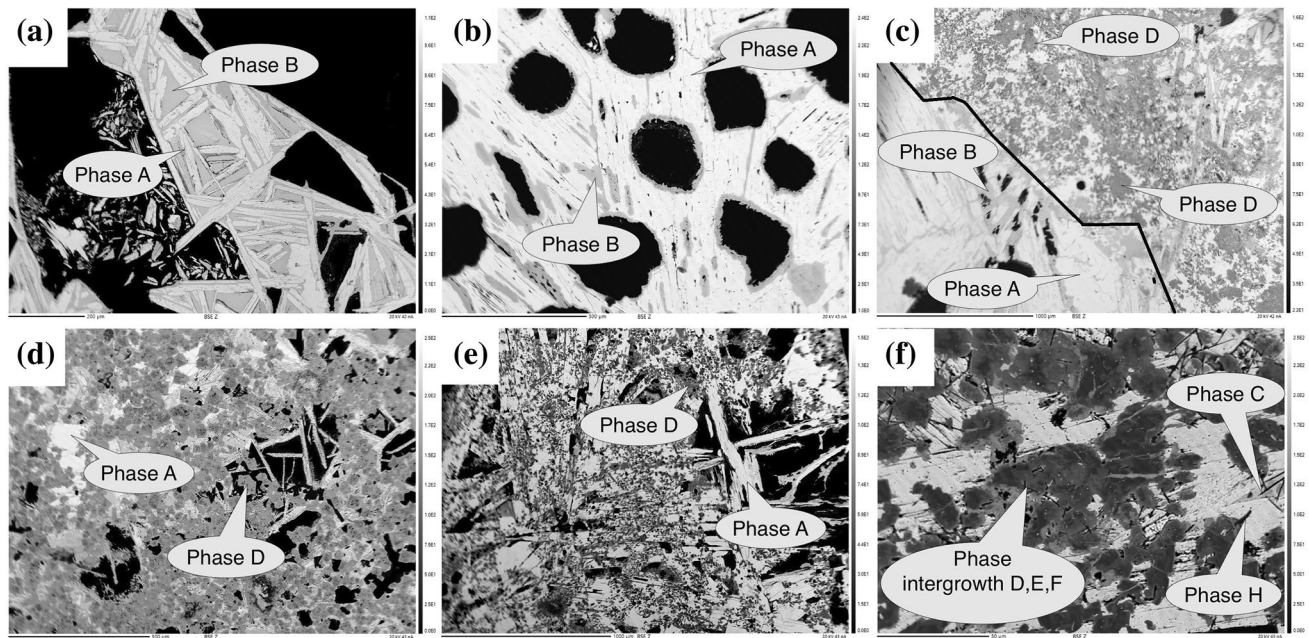


**Fig. 6** BSE images. (a) Lath-like white crystals of phase A in zone I (sample NA5). Phase B fills the interstices. (b) Crystals of phase A in zone I, phase B fills the open space of sample 67 and surrounds pores (black). (c) Boundary between zone I and II of sample 63b. Phase D is significantly dominant in zone II, phase A changes from lath-like to

acicular crystals. (d) Zone III of sample 63b with typical microstructure. (e) Sample 64. Acicular crystals of phase A in zone II. Phase D forms clusters. (f) Sample 53.2. Phase C, E, F and H. Phase E coexist with phase D. [Scale bars: (a) 200  $\mu\text{m}$ , (b) 500  $\mu\text{m}$ , (c) 1000  $\mu\text{m}$ , (d) 500  $\mu\text{m}$ , (e) 1000  $\mu\text{m}$ , (f) 50  $\mu\text{m}$ ]

(3.21 wt.%); CaO decreases from phase B to phase C (0.29 wt.% to 0.01 wt.%). Phase C occurs exclusively in zones III and IV of samples 5, 53 (53.2) from Cerro del Plomo and 63b, 64 and 67 from Fuente Espi.

### Ca–Si–Pb–O Phases

Four Ca–Si–Pb–O phases were observed in zones II, III and IV (Fig. 5). Based on the EPMA analyses and the derived statistics (25% quantile to 75% quantile) (Table 3), phase D, E, F, and G can be defined (Fig. 6). The most obvious is a decreasing PbO content from D to G (Fig. 5). Phase D is the most common of the four phases. In zones II and III, D is associated with phase A. Together they form the white–grey matrix. There is a tendency for the proportion of phase D to increase from zone II to zone III and zone IV, and zonation of the crystals is observed. Phase D occurs in various forms, either xenomorphic, as partially rounded particles, as rod-shaped to rectangular or squat crystals, or as clusters. Often, phase D fills the interstices of phase A and occurs in intergrowths with phase E, which is the second most abundant Ca–Si–Pb–O phase in samples NA5, 53 (53.1 and 53.2) from Cerro del Plomo and 63b, 64 and 67 from Fuente Espi. Phases F and G were observed less frequently. Phase F was observed in samples 63b, 64, 67,

and 53.2 (Fig. 6f), while phase G exclusively was observed in sample 67 from Fuente Espi.

### Si–Pb–O Phases with Variable K, Al, Mg, Ca

Phases dominated by Si, Pb and O and with more variable contents of K, Al, Mg and Ca can be identified in zones III and IV (phases H–M, Table 3 and Fig. 6).

### Ca–Pb–O Phase

In samples 53 (53.1, 53.2) from Cerro del Plomo and 63b and 67 from Fuente Espi, a further phase consisting of Ca, Pb, and O with a wide variation in lead content was identified. The phase is characterized by a cathodoluminescence effect.

### Metal Inclusions

Metal inclusions of copper and lead are co-existent. Metallic copper occurs in zones II–IV and predominantly in phases A or C. Copper inclusions are present as (hyp)idiomorphic crystals with resorption lacunae, and their size usually does not exceed 30  $\mu\text{m}$  (Figs. 7 and 8). Pure lead was identified as globular inclusions. They have diameters of  $\sim 25$ –200  $\mu\text{m}$  and are surrounded by phase A (PbO). The Cu and Pb

**Fig. 7** Metallic Cu-inclusions in zone IV of sample 64. The inclusions are encircled. **(a)** Cu inclusions with a striking reflection colour under reflected light. **(b)** backscattered electron image of the identical copper inclusions. The metallic Cu does occur within the phase C

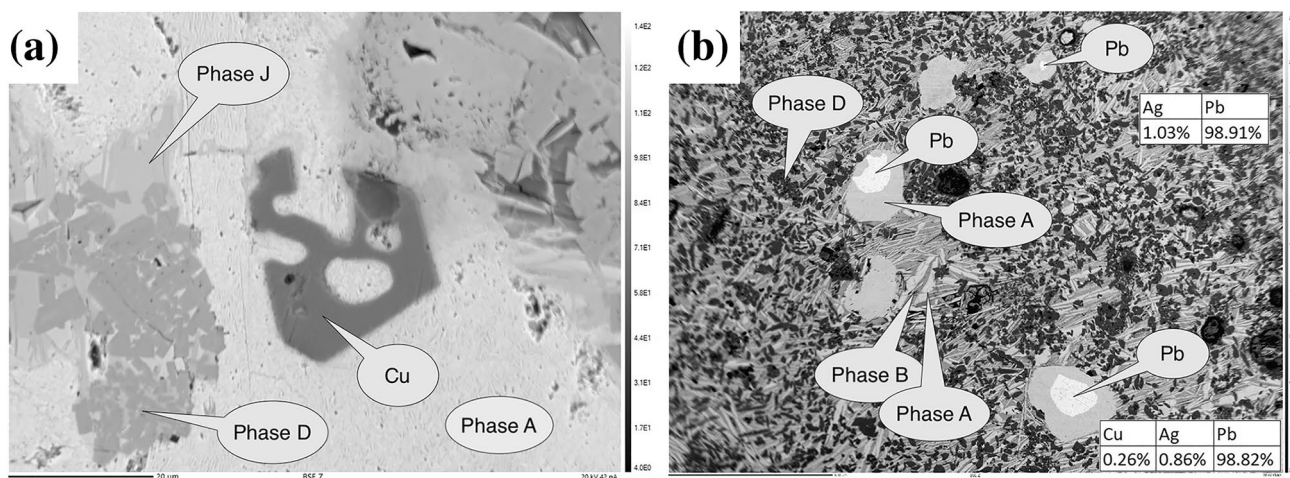
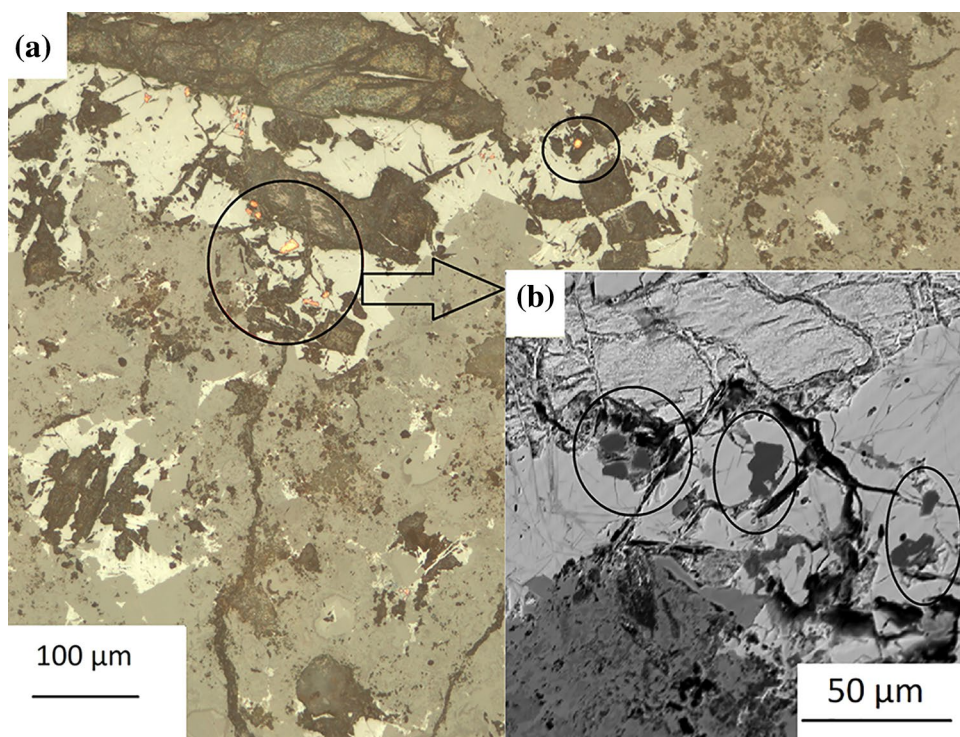


**Fig. 8** Backscattered electron images: **(A)** sample 53 (53.2). Idiomorphic Cu inclusion with resorption lagunae in phase A. **(b)** Metallic Pb (BSE white) inclusions are surrounded by PbO (BSE grey; phase A)

inclusions (Table 4 and Fig. 9) in the majority of samples do not contain detectable silver. Only Cu inclusions in sample 53.1 contain 580 ppm on average ( $n = 19$  single measurements), and Pb inclusions in sample NA5 contain 2030 ppm Ag on average ( $n = 10$  single measurements). Detectable Ni up to 0.3 wt.% only occurs in the metallic copper inclusions.

The co-occurrence of copper and lead inclusions here is a key to the temperature range under which they were formed. The (hyp)idiomorphous copper particles with resorption lacunae, allow the conclusion that they were exposed to

temperatures not much higher than the melting temperature of copper at 1083 °C. The fact that the lead inclusions are globular, i.e. that they were exposed to temperatures above the melting temperature of the lead, is not surprising.

### X-ray Diffraction of the Litharge Cakes

XRD analysis was performed to determine probable differences in mineralogical composition between the different zones and to distinguish between the different



**Table 4** EPMA analyses of the metal inclusions in the litharge samples from Cerro del Plomo and Fuente Espi

Sample	nb. spots analysed ( $n = x$ )	Inclusion type			Cu	Pb	Ag	Zn	Ni	Fe	Mn
		Cu	Pb	Cu-Pb							
Cerro del Plomo											
53-1	19	x			99.37	0.45	0.06	<0.03	0.10	<0.06	<0.02
53.2	30	x			99.65	0.22	<0.03	<0.03	0.13	<0.06	<0.02
NA5	10		x		<0.08	99.75	0.20	<0.03	<0.02	<0.06	<0.02
53.2	11		x		<0.08	99.97	<0.03	<0.03	<0.02	<0.06	<0.02
53.2	16			x	74.51	25.33	<0.03	<0.03	0.12	<0.06	<0.02
53.1	32			x	73.52	26.32	0.05	<0.03	0.09	<0.06	<0.02
Fuente Espi											
63b	7	x			99.59	0.19	<0.03	<0.03	0.20	<0.06	<0.02
64	14	x			99.08	0.50	0.03	<0.03	0.32	0.07	<0.02
67	32	x			99.51	0.18	<0.03	<0.03	0.30	<0.06	<0.02
63b	8		x		<0.08	99.96	<0.03	<0.03	<0.02	<0.06	<0.02
63b	1			x	88.15	11.64	<0.03	<0.03	0.20	<0.06	<0.02
64	19			x	75.66	23.20	0.03	<0.03	0.21	0.89	<0.02
67	5			x	63.52	36.20	<0.03	<0.03	0.26	<0.06	<0.02

modifications of Pb(II)O (Fig. 10). X-ray diffractograms of samples 53\_1 and 63b\_1 (zone IV; Fig. 10 a) show comparable phase composition. Ganomalite, a calcium-rich  $\text{Pb}_9\text{Ca}_6[(\text{Si}_2\text{O}_7)_3(\text{SiO}_4)_3]$ , can be identified. In nature, ganomalite is a rare calcium-lead silica mineral belonging to the sorosilicate group. It can form dull white to grey masses in association with phlogopite and calcite, also with macedonite, celsian, idocrase and carbonate [29]. Ganomalite has a wide stability range in the system  $\text{CaO-SiO}_2\text{-PbO}$  [30]. Massicot and litharge are only identifiable (when truly present) by a slight asymmetry in the main intensity of ganomalite at  $29^\circ 2\theta$ , which overlaps with the main intensity of massicot, and by an enhanced background signal in the main intensity region of litharge around  $28.6^\circ 2\theta$ . Ca-rich ganomalite is also a component in Zone III (samples 53\_2 and 63b\_2), but this time accompanied alongside much higher peak intensities of litharge, the tetragonal PbO modification. Massicot occurs subordinately with a weak peak intensity at about  $30^\circ 2\theta$ . Zone II (sample 53.3) and zone I (sample 53.4) are nearly coincident and differ only in peak intensity. Here, the predominant phase is litharge. Especially for the samples from zone I and II, but also for the two samples from zone III, it is important to point out the strongly increased 00 l intensities (001, 002) of the litharge compared to the theoretical intensities from the database. This is due to a preferential orientation in the powder samples prepared for XRD analysis of the optically observed lath-like to acicular crystals of zones I and II. Also, the significant decrease in the half-width of the 00 l intensities compared to the reflections from the other lattice directions could indicate an anisometric crystallite form. Massicot

is present only in minute amounts, and ganomalite is not detectable in Zone I. Cerussite, a lead carbonate phase, and calcite were identified in varying amounts in the samples from zones II-IV. Potentially, calcite contains some Mg, as indicated by a slight shift in the main intensity. Both minerals are presumably secondary products of alteration.

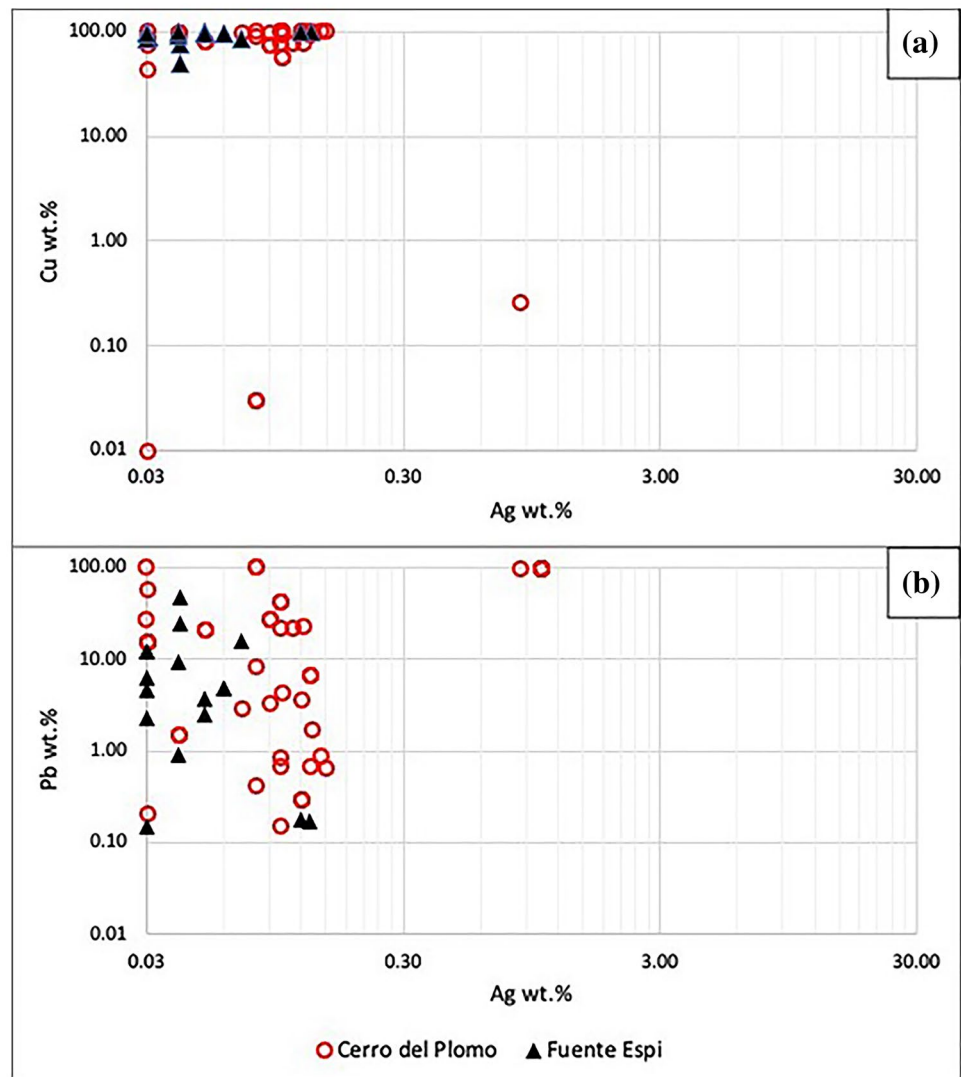
Neither the metal inclusions can be resolved by X-ray diffraction, nor is it possible to identify the different Si-Pb-O phases H-M. The Ca-Si-Pb-O phases (phases D-G) were identified as ganomalite in the diffractograms. The chemical differences of the phases distinguished under the microscope may be too small to identify them as individual species in the XRD.

## Discussion

The pyrometallurgically formed litharge cakes of Cerro del Plomo and Fuente Espi show a high-resolution stratigraphy, which can be subdivided into four zones. Most important is that the crystallization behaviour of the main phase of PbO varies: In the dark red zone I, it forms a framework of large lath-like crystals, which allows the crystallization of a Ca-Si-Pb phase only in the interstices. Pores have formed, presumably due to degassing of volatile components. The adjacent red zone II, separated from I by a sharp boundary, is also dominated by the main PbO phase, but here the crystals are acicular and much smaller. This allows precipitation of larger amounts of Ca-Si-Pb-O and Si-Pb-O phases. Zones III (reddish) and IV (yellow, brown-black) are also characterized by these phases, and PbO is difficult to



**Fig. 9** Bivariate diagrams. (a) Cu versus Ag in the copper inclusions. (b) Pb versus Ag in the lead inclusions [axis minimum limit Ag=D.L., logarithmic scaling, single point measurements by EPMA.]



differentiate. The yellow and reddish coloured areas of the litharge cakes visible to the naked eye can be explained by the XRD results. Litharge, the low-temperature modification of PbO, shows red internal reflections and therefore, appears red, while Massicot, the high-temperature phase, appears yellow. Litharge is predominant in the deep red or red areas, while massicot is predominant in the reddish to yellow–brown areas. Zone I is virtually all litharge, while massicot increases from Zone II to Zone IV. At the same time, the calcium-rich ganomalite phase increases, also visible under the microscope as grey masses in zones III and IV. The ganomalite signals in the XRD spectra may be representative of all Ca–Si–Pb–O phases present, which gradually differ from each other in chemical composition.

Two models for the formation of litharge during the cupellation process are described in the literature, one is the overflowing of the Pb–Ag melt with air, where the forming PbO is tapped off, the other is by the use of "hollow sticks" [5]. The litharge cakes of this study were clearly formed by the process of overflowing. In the cupellation furnace, the oxidized and liquid PbO, which floated on top of the molten lead–silver, was poured into crucibles or into a collecting pit outside the cupellation furnace. Pouring subjected the liquid to relatively fast cooling, as evidenced by the small size of the acicular PbO component in zones II–IV and the increasing presence of massicot: The metastable high-temperature phase is preserved through fast cooling. In contrast, the high pore volume as well as the extensively grown crystals of zone I, which has its sharp and distinct boundary with zones

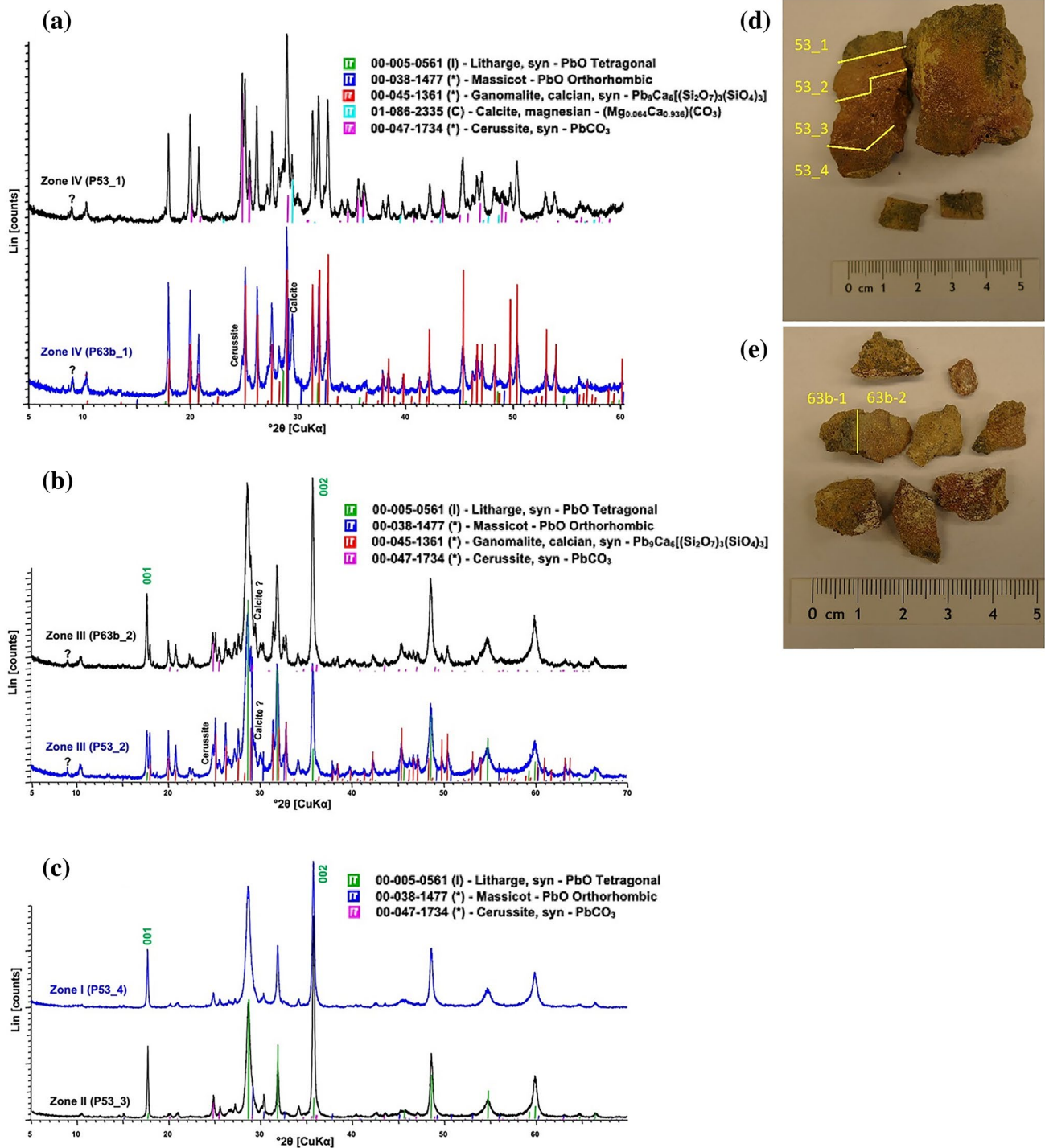


**Fig. 10** X-ray diffractograms of zones I, II-IV and identified phases. (a) Phases identified in zone IV (samples 63b\_1 and 53\_1). (b) Phases identified in zone III (samples 63b\_2 and 53\_2). (c) Phases

identified in zone I (sample 53\_4) and II (sample 53\_3). (d) Split of sample 53 for XRD measurements. (e) Split of sample 63b for XRD measurements

II-IV, indicate that this was previously a foam on top of the litharge-clay mass: the PbO crystals had sufficient space to grow and develop to large and lath-like crystals. This is also consistent with the dominance of the low-temperature

modification litharge in zone I, which re-modifies from the metastable high-temperature phase massicot.

The nature of the metal inclusions revealed that in addition to lead also copper was present in the system.

If detectable, silver could be determined in both copper and lead inclusions, whereas the copper also contains nickel. The presence of the high calcium content in the D-G phases indicates the use of a Ca-rich collection clay, as has been called for in the literature. Whether bone or plant ash was used needs further discussion. EPMA revealed up to 1.1 wt.% phosphorous in one of the litharge samples from Fuente Espi. But bulk geochemical analyses will be subsequently performed to verify the values. Envisaged is an extended chemical and isotopic characterization of the material. In a further step, the ore finds from the collection will also be comparatively analysed. The (electron) microscopic analyses did not reveal any differences between the Cerro del Plomo and the Fuente Espi litharge cakes. However, it remains to be seen if the geochemical analyses and the comparison with the ore finds will allow a further differentiation.

## Conclusion

Several litharge cake samples from two Roman foundry sites in the Spanish Sierra Morena were analysed by stereo and reflected light microscopy, XRD and EPMA to obtain elemental and phase characterization of the litharge and conclusions about the ore used. In addition, the study serves to compare the smelting processes carried out in the two foundries. The litharge samples are strongly stratigraphed. Within a cake, four compositional zones can be distinguished, with lead content being depleted from one to the other, while at the same time the silica- and calcium-rich phases, including Al, K, and Mg, increase. The different zones are visible to the naked eye by a colour change from dark red to brown–black, by phase analysis characterized by different PbO ratios of tetragonal litharge and orthorhombic massicot phase. Lead and copper are present as inclusions almost throughout the litharge cakes. Spherical lead testifies to the involvement of molten lead in the process. Hypidiomorphic to angular copper inclusions with resorption lacunae are relics of the only partially melted ore charge, indicating that the lead ore must have contained copper-rich accompanying phases that were associated with nickel according to elemental analysis. Whether crushed ore or concentrates were used in the foundries cannot be determined by examination of the litharge. In any case, the remaining gangue is removed in previous smelting steps in which the sulfidic material is converted to lead-silver. It is expected that the gangue material was previously converted to a slag.

The high-resolution stratigraphy of the litharge samples can be linked to the available theoretical models. The coincidence of stratigraphy and crystal size of the lead-rich

phases is evident. An overflowing process was performed in which air is blown over a lead-silver melt in a cupellation furnace and lead oxide is tapped into a separate container or mould. Due to high degassing, a foam forms on the top of the solidifying litharge cake, resulting in large lath-like lead-bearing crystals on the top of the cooling mass. As the crystals progressively grow into the cake, the crystal sizes continuously decrease and the crystal texture changes in favour of a fine-grained structure. Elemental and mineralogical interpretation shows that litharge cakes are not a homogeneous mass and therefore need to be examined only when complete. If only small pieces are provided for archaeometric analysis, the overall picture may be missed.

The two foundry sites, "Cerro del Plomo" and "Fuente Espi", from which the litharge samples were taken, are assigned differently to their potential ore deposits. While "Cerro del Plomo" is located opposite "Socavón Don Francisco" and is closely related to the rich vein of "El Centenillo", the ore deposit that fed the Fuente Espi process has not yet been discovered. However, analyses of litharge samples from the two sites show no significant differences in microstructure, phase composition or stratigraphy. The planned continuation of the study on the remaining foundry material, including ore, slag, and lead metal finds, will provide a more complete picture of the two sites.

**Acknowledgements** The topic is related to a work package within the Excellent Science-ERC project "Silver Isotopes and the Rise of Money" by Francis Albarède, Lyon. The study is part of a dissertation by the first author of this paper (P. Krause). This is paper No. 1. The PhD position were financed by the Deutsches Bergbau-Museum Bochum. We thank Sandrine Baron, Lyon for providing access to Claude Domerque's collection. The Deutsches Bergbau-Museum financially supported the analyses. The Ruhr-Universität Bochum provided access to their electron microprobe facilities. Our thanks go to Sandra Kruse called Lüttgen in the preparation laboratory of the German Mining Museum Bochum for sample preparation and polished sections, and to Hannah Zietsch, Archaeometallurgy Research Unit, for redrawing the trivariate diagram. We appreciate the helpful comments of the anonymous reviewers and the help of the editor, based on which we were able to improve the manuscript even further.

**Funding** Open Access funding enabled and organized by Projekt DEAL.

**Open Access** This article is licensed under a Creative Commons Attribution 4.0 International License, which permits use, sharing, adaptation, distribution and reproduction in any medium or format, as long as you give appropriate credit to the original author(s) and the source, provide a link to the Creative Commons licence, and indicate if changes were made. The images or other third party material in this article are included in the article's Creative Commons licence, unless indicated otherwise in a credit line to the material. If material is not included in the article's Creative Commons licence and your intended use is not permitted by statutory regulation or exceeds the permitted use, you will need to obtain permission directly from the copyright holder. To view a copy of this licence, visit <http://creativecommons.org/licenses/by/4.0/>.



## References

1. S.W. Merkel, The richness of silver ore in the middle ages: a comparative study of historical descriptions and the archaeological evidence. *Der Anschnitt, Beih.* **45**, 39–44 (2020)
2. C.J. Paterson, Ore deposits of gold and silver. *Miner. Process. Extr. Metall. Rev.* **6**(1–4), 43–66 (1990). <https://doi.org/10.1080/08827509008952656>
3. Cogram, P.F.: Capacity and mechanisms of uptake of silver by Jarosite family minerals. Thesis for the degree of Doctor of Philosophy. University of London (2016)
4. H. Lechtman, S. Klein, The production of copper-arsenic alloys (arsenic bronze) by cosmelting: modern experiment, ancient practice. *J. Archaeol. Sci.* **26**, 497–526 (1999)
5. T. Rehren, D. Vanhove, H.F. Mussche, M. Oikonomakou, Litharge from Laurion. A medical and metallurgical commodity from South Attika. *Antiq.* **68**(1), 299–308 (1999). <https://doi.org/10.3406/antiqu.1999.1348>
6. Berger, D.: Steingußformen aus dem spätromischen-frühgotischen Magdeburg. Diploma Thesis, Available from Freiberg (Sachsen), 2006. Thesis completed September, 2005.
7. E. Gliozzo, C. Ionescu, Pigments - lead-based whites, reds, yellows and oranges and their alteration phases. *Archaeol. Anthropol. Sci.* **14**(1), 17 (2022). <https://doi.org/10.1007/s12520-021-01407-z>
8. Y. Wang, X. Lin, H. Zhang, T. Wen, F. Huang, Y. Wang, F. Liao, J. Lin, Selected-control hydrothermal growths of  $\alpha$ - and  $\beta$ -PbO crystals and orientated pressure-induced phase transition. *Cryst. Eng. Comm.* **15**(18), 3513–3516 (2013). <https://doi.org/10.1039/C2CE26162F>
9. R. Blanchard, The interpretation of leached outcrops. Nevada Bureau Mines. Bulletin. **66**, 212 (1968)
10. B. Girbal, Roman and medieval litharge cakes: a scientific examination. *Research Report Series.* **51**, 1–80 (2011)
11. C. Milton, Llama bones with lead-copper mineralization from Bolivia. *Am. Miner.* **40**, 770–771 (1955)
12. C.G.I. Friedlaender, K. Choo, Mineralogical observations on slags from Zawar mines, Rajasthan. *Indian Mineral.* **11**, 1–10 (1970)
13. Oudbashi, O., and Wanhill, R., Archaeometallurgy of copper and silver alloys in the old world: ancient metals production and processing 179 (5), 24–27 (2021)
14. Conophagos, C. E.: *Le Laurion Antique et la Technique Grecque de la Production del' Argent, Ekdotike Hellados.*, Athens, Greece (1980)
15. Bachmann, H. G.: The archaeometallurgy of silver. In: *Archeologia delle attivita estrattive e metallurgiche* pp. 487–495 (1993)
16. Bayley, J., Eckstein, K.: Roman and medieval litharge cakes: structure and composition, In J. Pérez-Arantegui (ed), *Proceedings of the 34th international symposium on archaeometry, Zaragoza, 3–7 May 2004*, 145–153 (2006).
17. Bayley, J.: The discovery of precious metal refining in Roman Chicester. In: *Proceedings of the 36th international symposium on Archaeometry, Québec City, Canada*, 425–431 (2006)
18. M. Martínón-Torres, N. Thomas, T. Rehren, A. Mongiatti, Some problems and potentials of the study of cupellation remains: the case of post-medieval Montbéliard, France. *Archeosciences.* **32**, 59–70 (2008). <https://doi.org/10.4000/archeosciences.948>
19. Th. Rehren, Alchemy and fire assay – an analytical approach. *Hist. Metall.* **30**, 136–142 (1996)
20. Gauthier, J., Téreygeol, F.: Small scale reduction of argentiferous galena: first experimental approach to ores assaying techniques. In D Dungworth and R C P Doonan (eds) *Accidental and Experimental Archaeometallurgy*, 8, London (2013)
21. J. Percy, *The metallurgy of lead including desilverisation and cupellation* (John Murray, Albemarle Street, London, 1870)
22. M.A. Worthing, H.H. Sutherland, The composition and origin of massicot, litharge (PbO) and a mixed oxide of lead used as a traditional medicine in the Arabian Gulf. *Miner. mag.* **60**(400), 509–513 (1996). <https://doi.org/10.1180/minmag.1996.060.400.12>
23. D.L. Perry, T.J. Wilkinson, Synthesis of high-purity  $\alpha$ - and  $\beta$ -PbO and possible applications to synthesis and processing of other lead oxide materials. *Appl. Phys. A.* **89**(1), 77–80 (2007). <https://doi.org/10.1007/s00339-007-4073-y>
24. I.J. Lin, S. Niedzwiedz, Kinetics of the Massicot-Litharge transformation during comminution. *J. Am. Ceram. Soc.* **56**(2), 62–64 (1973). <https://doi.org/10.1111/j.1151-2916.1973.tb12358.x>
25. C. Domergue, El Cerro del Plomo, mina El Centenillo (Jaén). *Noticiario Arqueológico Hispánico.* **16**, 265–380 (1971)
26. Domergue, C.: *Catalogue des mines et des fonderies antiques de la Péninsule Ibérique. Publications de la Casa de Velázquez, série Archéologie VIII (tome I)*, 264–276 (1987)
27. C. Domergue, Les mines de la Péninsule Ibérique dans l'Antiquité romaine. *Collection de l'École française de Rome.* **127**, 261–262 (1990)
28. Berthold, C., Keuper, M., Bente, K.: Dealing with antique objects: Non-destructive X-ray microdiffraction coupled with  $\mu$ -Raman spectroscopy and  $\mu$ -X-ray fluorescence. In: *Archäometrie und Denkmalpflege 2015*, 7, 24–26 (2015)
29. P.J. Dunn, D.R. Peacor, J.W. Valley, C.A. Randall, Ganomalite from Franklin, New Jersey, and Jakobsberg, Sweden: new chemical and crystallographic data. *Miner. Mag.* **49**(353), 579–582 (1985). <https://doi.org/10.1180/minmag.1985.049.353.12>
30. M. Shevchenko, E. Jak, Experimental Liquidus study of the binary PbO-CaO and ternary PbO-CaO-SiO<sub>2</sub> systems. *J. Phase Equilib. Diffus.* **40**(2), 148–155 (2019). <https://doi.org/10.1007/s11669-019-00705-3>

**Publisher's Note** Springer Nature remains neutral with regard to jurisdictional claims in published maps and institutional affiliations.